Published in final edited form as:
J Mol Neurosci. 2011 September ; 45(1): 32–41. doi:10.1007/s12031-011-9502-x.

Proteasome Inhibition Drives HDAC6-Dependent Recruitment of Tau to Aggresomes

Chris R. Guthrie and
Geriatrics Research Education and Clinical Center, Veterans Affairs Puget Sound Health Care System, Seattle, WA 98108, USA

Brian C. Kraemer
Geriatrics Research Education and Clinical Center, Veterans Affairs Puget Sound Health Care System, Seattle, WA 98108, USA

Division of Gerontology and Geriatric Medicine, Department of Medicine, University of Washington, Seattle, WA 98104, USA

Seattle Veterans Affairs Puget Sound Health Care System, S182 1660 South Columbian Way, Seattle, WA 98108, USA

Brian C. Kraemer: kraemerb@uw.edu

Abstract

Lesions containing aggregated and hyperphosphorylated tau protein are characteristic of neurodegenerative tauopathies. We have developed a cellular model of pathological tau deposition and clearance by overexpressing wild type human tau in HEK293 cells. When proteasome activity is inhibited, HEK293/tau cells accumulate tau protein in structures that bear many of the hallmarks of aggresomes. These include recruitment of tau into large spherical inclusions, accumulation of the retrograde motor protein dynein at the centrosome, formation of an intermediate filament cage around inclusions, and clustering of mitochondria at the aggresome. Tau aggresomes form rapidly and can be cleared upon relief of proteasome inhibition. We observe recruitment of pathological misfolded phospho-tau species to aggresomes. Immunoblotting reveals accumulation of detergent insoluble aggregated tau species. Knockdown of histone deacetylase 6, a protein known to interact with tau, reveals a requirement for HDAC6 activity in tau aggresome formation. Direct observation of the accumulation and clearance of abnormal tau species will allow us to dissect the cellular and molecular mechanisms at work in clearing aggresomal tau and its similarity to disease relevant pathological tau clearance mechanisms.

Keywords

HDAC6; Aggresome; Tau; Protein aggregation; Proteasome; Tauopathy

Introduction

Dementia disorders caused by neurodegenerative changes often display accumulation of various forms of aggregated tau protein. Tau lesions occur upon neuropathological

Correspondence to: Brian C. Kraemer, kraemerb@uw.edu.

Electronic supplementary material The online version of this article (doi:10.1007/s12031-011-9502-x) contains supplementary material, which is available to authorized users.

examination in virtually all cases of Alzheimer's disease (AD), FTLD-tau, Guam ALS/PDC, Pick's disease, progressive supranuclear palsy, and corticobasal degeneration (reviewed in Gendron and Petrucelli 2009; Alonso et al. 2008). Likewise protein aggregation is a recurring theme in the pathology of diverse neurodegenerative disorders. A subset of these diseases, including AD, manifests abnormal lesions where the microtubule binding protein tau has been identified as the main component. Specifically in AD, neurofibrillary tangles (NFT) and neuropil threads contain insoluble deposits of hyperphosphorylated tau. Normal tau binds to tubulin and promotes microtubule (MT) formation and stability in neuronal axons. MTs function as an essential component of the cytoskeleton and are crucial for maintenance of neuronal morphology and cellular trafficking activities. Disruption of normal tau function may cause cellular toxicity by destabilizing MTs (Hong et al. 1998; Barghorn et al. 2000) or by promoting tau aggregation (Hong et al. 1998; Barghorn et al. 2000; Goedert et al. 1999; Arrasate et al. 1999).

The mechanism by which abnormal tau can be degraded or detoxified by the cell remains incompletely understood (reviewed in Johnson 2006). However, both the ubiquitin–proteasome system (UPS; Shimura et al. 2004; Kosik and Shimura 2005) and the macroautophagy pathway (Wang et al. 2010) have been implicated in tau turnover. Furthermore, both the UPS and lysosomal systems have been demonstrated to be disrupted in AD and may also be dysfunctional in other disorders exhibiting tau pathology (Wang et al. 2009; Boland et al. 2008; Nixon 2007). Fibrillar tau species have also been demonstrated to directly inhibit proteasome activity (Keck et al. 2003).

In order to further dissect the cellular mechanisms operating to clear pathological tau species, we have explored the effects of proteasome inhibition on tau aggregation and clearance. We have generated a cellular model of tau pathology relying on proteasome inhibition rather than tau mutations to drive the formation of pathological tau species. The resulting cellular model exhibits hallmark features of early tau pathology seen in AD and other tauopathies, namely increased protein aggregation and abnormal phosphorylation of tau. This model system will allow further characterization of wild-type tau aggregation and toxicity and provide a system to rapidly test different neuroprotective strategies and to test hypotheses regarding tau neurotoxicity.

Materials and Methods

Plasmids and Cells

A stable cell line (HEK/tau) overexpressing wild-type human tau (4R1N) was constructed by adding linkers to the tau cDNA and inserting into the MCS of pcDNA3.1 zeo$^{(-)}$ at XhoI/EcoRI. HEK293 (ATCC catalog # CRL-1573) cells were transfected with this plasmid using GenePORTER H (Genlantis). HEK293 cells were used as the parental cell line due to their ease of use and the fact that they share many properties with immature neurons (Shaw et al. 2002). Antibiotic-resistant clones were selected with 100 μg/mL as Zeocin. Clones expressing high amounts of tau were screened using immunofluorescent microscopy and confirmed by immunoblotting.

Cell Culture and Drug Treatments

HEK/tau cells were cultured under standard culture conditions (Dulbecco's modified Eagle's medium, 10% defined fetal bovine serum, penicillin (50 IU/mL) − streptomycin (50 μg/mL) + Zeocin (100 μg/mL)) to maintain selection. For proteasome inhibition, proteasome inhibitor I (PSI) was added to a final concentration of 2 μg/mL for 18 h. Also tested were lactacystin (5 μM) and MG132 (1 μM). RNAi experiments were carried out as recommended by the manufacturer (IDT). Cells were analyzed 48–72 h post-siRNA

treatment. HDAC6 duplex sequences: 5′-GGAGAG GAGAACCUAGGAGAGG-3′; 3′-GUCCUCUCCUCUUGGAUGAUCCUCUCC-5′.

Immunocytochemistry

HEK/tau cells grown on poly-D-lysine-coated 12-mm round coverslips were fixed in 4% formaldehyde. Cells were washed 3×5 min in phosphate-buffered saline (PBS)/Ca^{2+}/Mg^{2+} and then blocked in antibody buffer (PBS, 0.5% Triton X-100, 1 mM EDTA, 0.1% bovine serum albumin, 0.05% NaN_3)+10% normal goat serum. Primary antibodies were applied and incubated for 1 h at room temperature. Cells were washed 3×5 min in PBS/Ca^{2+}/Mg^{2+} and then reblocked for 10 min. Appropriate secondary antibodies were applied and incubated for 20 min at room temperature. Cells were again washed 3×5 min in PBS/Ca^{2+}/Mg^{2+}, counterstained with 300 nM DAPI, and mounted with ProLong Gold antifade (Molecular Probes).

Antibodies for Immunostaining

Anti- tau antibodies used include rabbit polyclonal 17025 (IF 1:1,000; WB 1:6,000; a gift from Virginia Lee), T46 (IF 1:1,000), 12E8 (IF 1:200; a gift from Peter Seubert), PHF-1 (IF 1:200; a gift from Peter Davies), Tau-2 (IF 1:1,000; Sigma), Alz50 (IF 1:100; a gift from Peter Davies), Vimentin (IF 1:100; Abcam), HDAC6 (IF 1:50, WB 1:1,000; Abcam), dynein (Millipore; IF 1:500), and α-tubulin (IF 1:1,000; WB 1:1,000).

Microscopy, Image Acquisition, and Processing

Microscopy was performed on a Nikon Eclipse TE300 epifluorescent microscope. Images were acquired using a Photometrics SenSys™ cooled CCD camera and IPLab image acquisition software (BD Biosciences Bioimaging). Images were deconvolved using MicroTome™ deconvolution software (BD Biosciences Bioimaging). Image processing with Adobe Photoshop consisted of histogram stretch, noise removal with Despeckle filter, and sharpening using Unsharp Mask (50%, 3 pixel radius).

Tau Protein Extraction and Immunoblotting

Tau fractions were obtained as described (Ishihara et al. 1999; Guthrie et al. 2009). To analyze detergent insoluble tau accumulation, HEK293 cell pellets were sequentially extracted using buffers of increasing solubilizing strength. HEK293/tau cells were homogenized in high salt reassembly buffer (RAB-High Salt (0.1 M MES, 1 mM EGTA, 0.5 mM $MgSO_4$, 0.75 M NaCl, 0.02 M NaF, 0.5 mM phenylmethylsulfonyl fluoride (PMSF), 0.1% protease inhibitor cocktail, pH 7.0)) and ultracentrifuged at 50,000×*g* yielding the soluble fraction (supernatant) and an insoluble pellet. Next, the RAB insoluble material was re-extracted with an ionic and non-ionic detergent containing RIPA buffer (50 mM Tris, 150 mM NaCl, 1% NP40, 5 mM EDTA, 0.5% DOC, 0.1% sodium dodecyl sulfate (SDS), 0.5 mM PMSF, 0.1% protease inhibitor cocktail, pH 8.0) and centrifuged as above yielding abnormal tau in the supernatant. Finally, the detergent insoluble pellet was re-extracted with 70% formic acid (FA) to solubilize detergent insoluble tau. The three fractions were analyzed by immunoblotting. Protein samples were boiled 5 min and loaded onto 4–15% pre-cast Critereon SDS–polyacrylamide gel electrophoresis gradient gels (Bio-Rad). For immunoblotting, we detected human tau using antibody 17025 at a dilution of 1:6,000 (A generous gift from Virginia Lee) as described previously (Guthrie et al. 2009). We used anti-tubulin antibody at a dilution of 1:1,000 (Developmental Studies Hybridoma Bank). Secondary goat anti-mouse or goat anti-rabbit IgG was the secondary antibody reagents used at a dilution of 1:1,000 (GE Lifesciences). Signals were measured by densitometry using Adobe Photoshop.

Results

Proteasome Inhibition Drives Tau into Aggresomes

Wild-type tau protein accumulates in the NFTs and other tau-containing deposits seen in Alzheimer's disease (reviewed in Trojanowski and Lee 2002; Gotz et al. 2008). In order to study the accumulation of non-mutated wild-type tau into aggregates, we chose to develop a model of tau expression in HEK293 cells. HEK293 cells share many similarities to immature neurons but are more easily transfected (Shaw et al. 2002). Normal endogenous human tau is expressed at low but detectable levels in HEK293 cells using the pan tau antibody T46 and immunofluorescence microscopy (Fig. 1a). To model the aggregation and turnover of tau, we generated stable HEK293 cell lines expressing high levels of wild-type human tau (Fig. 1b). Tau isoform 4R1N was chosen because it is the most abundantly expressed isoform in the human brain. High level expression of tau protein is sufficient to drive the formation of tau-positive structures with the morphology of aggresomes in a small fraction of HEK293/tau cells suggesting tau-containing aggresomes may form in response to increased tau concentration (data not shown); we used proteasome inhibition to increase tau aggresome formation as previously described (Ding et al. 2008).

Treatment of either HEK293 or HEK/tau cells overnight (18 h) with PSI, a reversible inhibitor of the chymotrypsinlike activity of the proteasome (Traenckner et al. 1994), causes tau protein to accumulate in a spherical peri-nuclear structure resembling an aggresome (Fig. 1c, d; Johnston et al. 1998). Spherical deposits are also induced by other proteasome inhibitors acting through distinct mechanisms (see Fig. S1), including lactacystin which blocks proteasome activity by covalently modifying the catalytic β-subunit of the proteasome (Imajoh-Ohmi et al. 1995) and MG-132 which acts by simultaneously increasing the activity of the β2 subunit will reducing the activity of other β subunits of the 26S complex (Tsubuki et al. 1996).

HEK/Tau Cells Form Large Aggregates with Characteristics of Aggresomes

Accumulation of abnormally oxidized or aggregated proteins leads to formation of the aggresome (reviewed in Olzmann et al. 2008). By treating HEK/Tau cells with 2 μM PSI, we were able to drive tau to aggregate in structures with the hallmarks of aggresomes (Fig. 2). Shown is a representative single cell stained for normal human tau (Fig. 2a). The majority of tau protein has moved to the aggresome at the microtubule organizing center (MTOC). Also note the deformation of the nuclear envelope by the deposited aggregated protein. Immunostaining of identically treated cells (Fig. 2b) reveals a cage-like structure formed by the intermediate filament protein, vimentin, a characteristic of aggresomes in cultured non-neuronal cells (Johnston et al. 1998). Likewise, when proteasome activity is inhibited, the retrograde motor protein dynein, which is required for transport of proteins to the aggresome (Yoshiyama et al. 2007; Iwata et al. 2005a), can be seen here clustered about the centrosome (Fig. 2c). In addition, we have observed that treatment with proteasome inhibitor causes mitochondria (observed by staining live cells with MitoTracker Red) to reorganize and cluster around the periphery of the aggresome as seen here (Figs. 2d and 3) and in (Debure et al. 2003). Finally, Fig. 2e demonstrates contraction of the microtubule network to bundle around the tau-containing aggresome and the nucleus.

Aggresomes Containing Tau Form Rapidly and Reversibly upon Proteasome Inhibition

In order to investigate the temporal relationship between proteasome inhibition and aggresome formation, we prestained mitochondria in live HEK/tau cells with MitoTracker dye. Recent work has demonstrated a role for mitochondria in the formation of aggresomes/autophagosomes (Boeddrich et al. 2003; Hailey et al. 2010). The observation that mitochondria are recruited to the periphery of tau-containing aggresomes (Fig. 2d) allowed

real-time tracking of tau aggresome formation in live HEK/tau cells by observing stained mitochondria. In as little as 1 h, the mitochondria began to redistribute (Fig. 3a). After 3 h, the majority of mitochondria had translocated to positions near the nucleus, and a few nascent aggresomes were observed. Nine hours after initiation of proteasome inhibition, fully formed aggresomal structures were observed in nearly every cell. Clearance of aggresomes was monitored in live cells by disappearance of mitochondria cluster around the MTOC and the reestablishment of a normal mitochondrial network throughout the cytoplasm. This process was evident first as breakdown of the mitochondrial cluster around the mature aggresome 18 h following washout of proteasome inhibitor and is complete after 42 h of recovery (Fig. 3b).

Pathological Tau Accumulates in Aggresomes

Tau epitopes seen in the neuropathology of AD become concentrated within aggresomes in HEK/tau cells (Fig. 4). In Fig. 4, we show immunostaining with the phospho-specific antibodies 12E8 (phospho-Ser262; Seubert et al. 1995; Fischer et al. 2009) and PHF-1 (phospho-Ser396/404; Evans et al. 2000), along with conformation specific antibodies Alz50 and Tau-2. Phosphorylation of tau at Ser262 (the 12E8 site) in the microtubule binding repeat domain R1 results in a bend in the tau molecule which precludes microtubule binding, resulting in free tau (Fischer et al. 2009; Biernat et al. 1993). This free tau is then available for hyperphosphorylation at other epitopes, such as PHF-1 (Ser396/404). Antibodies 12E8 (Fig. 4a, b) and PHF-1 (Fig. 4c, d), label epitopes seen in neurofibrillary lesions in AD, are translocated to the aggresome when proteasome activity is inhibited. The Alz50 antibody (Fig. 4e, f) recognizes a discontinuous epitope consisting of residues at the N terminus and the MT binding domains. It is suggested that this folded confirmation allows for intra-molecular interactions and formation of fibrillar tau (Carmel et al. 1996). While abundant ALZ50 staining is evident in non-treated cells, ALZ50 reactivity becomes localized to the aggresome upon proteasome inhibition. Tau-2 antibodies have high affinity for diverse aggregated tau species and label a variety of tau lesions in disease. Note that tau expressed in HEK/tau cells assumes the Tau-2 conformation only upon inhibition of the proteasome and formation of aggresomes (Fig. 4g, h).

Aggresome Formation Increases Levels of Detergent Insoluble Tau

Detergent insolubility is one of the biochemical markers of pathological tau protein in Alzheimer's disease and other tauopathies. Similarly, in HEK/tau cells, wild-type tau protein accumulates in detergent insoluble aggregates. To examine the effects of proteasome inhibition on detergent insoluble tau, we treated HEK/tau cells with PSI and compared them to untreated cells. To extract soluble and insoluble tau fractions, we initially extracted HEK/tau cells in RAB, a high salt buffer, yielding the soluble tau fraction. We re-extracted material insoluble in RAB with RIPA, an ionic and non-ionic detergent containing buffer yielding the detergent soluble fraction. Subsequently, we recovered detergent insoluble material by extraction with formic acid (Fig. 5). In this sequential extraction experiment, we observe a modest increase in detergent insoluble tau in PSI-treated cells but little change in the soluble tau fraction relative to untreated HEK/tau cells.

HDAC6 Regulates Tau Aggresome Formation

HDAC6 has been shown to regulate aggresome formation by serving as a link between misfolded protein cargo and microtubules and is necessary for aggresome formation (Kawaguchi et al. 2003). We observe HDAC6 being recruited to tau-containing aggresomes (Fig. S2). To examine the functional role of HDAC6 in the formation of aggregated tau species, we reduced HDAC6 function in our HEK/tau model and examined the effect on detergent insoluble tau under conditions that do or do not form tau-containing aggresomes. In HEK/tau cells treated with siRNA targeting HDAC6, we see an approximately 75%

reduction in HDAC6 levels (Fig. 6a). This is accompanied by little change in high salt (RAB, lane 2) and detergent soluble (RIPA, lane 2) tau fractions. However, HDAC6 knockdown has a profound and context-dependent effect on insoluble tau species. Knockdown of HDAC6 in HEK/tau cells without aggresomes (normal proteasome activity) essentially eliminates detergent insoluble (FA, lane 2) tau (reduction >10-fold in HDAC6 RNAi treated HEK293/tau). In contrast, proteasome inhibition reverses this effect as knockdown of HDAC6 in HEK/tau cells with an inhibited UPS increases detergent insoluble tau species by ~250% (FA, lane 4). Figure 6b shows HEK/tau cells double stained for HDAC6 and tau. In the absence of HDAC6 knockdown, tau is trafficked to the aggresome along with much of the HDAC6 as observed previously (Fig. 6b). When HDAC6 is knocked down, no apparent change in the distribution of tau protein is observed. In contrast, when the UPS is inhibited during HDAC6 knockdown, redistribution of tau protein to the aggresome is impaired, and clearance of insoluble tau is hindered (Fig. 6a).

Discussion

Aggregated tau species are a key feature in AD and other neurodegenerative tauopathies. Precisely which tau species are the most neurotoxic remains unclear although a diverse array of phosphorylated, truncated, and aggregated species have been suggested (reviewed in Gotz et al. 2008). Aggresomes are hypothesized to be a repository for accumulation and clearance of misfolded, aggregated proteins, and thus likely a neuroprotective mechanism. Here we present a cellular model for the formation of tau-containing aggresomes and subsequent clearance of aggregated tau. HEK/tau cells which overexpress wild-type 4R1N human tau are induced to form abundant aggresomes by inhibition of the UPS (Fig. 1). When proteasome activity is inhibited, HEK/tau cells display many hallmarks of aggresome formation. These include migration to and accumulation of insoluble tau at the MTOC, deformation of the nuclear envelope, concentration of the retrograde motor protein dynein at the MTOC, formation of a vimentin cage surrounding aggregated protein, and migration of mitochondria to enclose the tau aggresome (Fig. 2). This process is rapid, occurring within a few hours of proteasome inhibition, and is reversible upon cessation of proteasome inhibition (Fig. 3). Together, these findings suggest that the aggresome is an alternate pathway for degradation and removal of potentially toxic tau aggregates. Furthermore, aggresome formation may be particularly relevant to AD, Pick’s disease, and other tauopathy disorders. Aggregated proteins are not efficient substrates for the proteasome, and PHF tau actually drives UPS dysfunction and decreased UPS activity (Keck et al. 2003; David et al. 2002). Regardless, wild-type tau aggregates as a result of UPS failure which is self-reinforcing because aggregated tau also further impairs UPS function (reviewed in Oddo 2008).

We examined the accumulation of abnormal tau species in our HEK/tau model. In this model, we see evidence for accumulation of hyperphosphorylated tau associated with pathological tau-positive lesions in AD and other tauopathies (Fig. 4, 12E8 and PHF1 staining). Likewise, we see obvious accumulation of abnormal tau conformers indicative of pre-tangle tau species (Fig. 4, Alz50 and Tau2 staining). With both hyperphosphorylated and aberrantly folded tau-positive staining, abnormal tau species are enriched in aggresomes (Fig. 4b, d, f, h). Furthermore, PSI treatment potentiates accumulation of detergent insoluble tau (Fig. 5). This finding supports the idea that abnormal tau species are preferentially recruited to aggresomes as they form, suggesting an important role for proteasome inhibition and autophagy-mediated degradation in tau-mediated pathologic mechanisms.

To explore the mechanistic relationship between aggresome formation and pathological tau species, we examined the functional importance of HDAC6 in turnover of insoluble tau because HDAC6 has been demonstrated to play an essential role in aggresome formation.

Also, HDAC6 has previously been shown to be increased in AD (Ding et al. 2008). HDAC6 is thought to participate in aggresome formation by increasing the efficiency of transport of aggregated proteins to the aggresome (Kawaguchi et al. 2003; Iwata et al. 2005b) and by binding to tau (Perez et al. 2009; Ding et al. 2008). We find that HDAC6 protein clearly overlaps with abnormal tau in aggresomes (Fig. S2) and alters the accumulation of aggregated tau species (Fig. 6). Taken together, these observations suggest that HDAC6 is associated with clearance of abnormal toxic tau. We hypothesize that HDAC6 normally promotes removal of insoluble tau from the cytoplasm via aggresome formation. In support of this, knockdown of HDAC6 dramatically reduces aggresomal accumulation of insoluble tau. Knockdown of HDAC6 along with proteasome inhibition produces a large increase in insoluble tau in the FA fraction. (Fig. 6) This appears counterintuitive at first glance. A possible explanation is that even though little aggregated tau is being transported to the aggresome for clearance, considerable aggregated tau is accumulating in the cytoplasm resulting in potentially greater toxicity under these conditions.

This hypothesis is also consistent with findings in other models, where HDAC6 function is inhibited by tau (Perez et al. 2009), perhaps by its direct interaction with tau (Ding et al. 2008). In other tau cellular models, mutations, fibrilization agents, and/or high levels of induced tau have been used to drive tau aggregation and toxicity (Bandyopadhyay et al. 2007; Wang et al. 2010; Khlistunova et al. 2006). Here we promote the formation of pathological tau aggregates using expression of normal human tau and pharmacological inhibition of proteasome activity. This mimics the proteasome dysfunction seen in AD (reviewed in Oddo 2008) and drives accumulation of abnormal tau species. Effects of proteasome inhibition on tau accumulation have been investigated previously in neuroblastoma SHSY-5Y cells (Hamano et al. 2009) and oligodendroglial (OLN-93) cells (Goldbaum et al. 2003). In both cellular models, proteasome inhibition promoted tau aggregation, consistent with what we observe here (Goldbaum et al. 2003; Hamano et al. 2009).

The cellular model described here has utility for dissecting the mechanisms employed by the cell for clearance of abnormal tau aggregates. The notion that tau can form aggresomes is particularly provocative because neurons seen in Pick's disease contain spherical tau deposits that at least superficially resemble aggresomes. Furthermore, we demonstrate here that HDAC6, a protein previously implicated in AD and turnover of aggregated proteins, plays a multi-faceted role in the genesis and degradation of abnormal tau aggregates. The tauopathy-related pathologic changes in this model are sufficiently robust for high-throughput screening for compounds that may prevent tau-related aggregation or toxicity.

Acknowledgments

This work was supported by a Department of Veterans Affairs Merit Review Grant (B.C.K.) and by National Institute of Neurological Disorders and Stroke Grant R01 NS064131 (B.C.K.) We thank Pam McMillan for critical reading of the manuscript. We thank the anonymous reviewers for their critical reviews and advice which helped improve this manuscript. We thank Elaine Loomis and Susan Danner for outstanding technical assistance. We thank Peter Davies, Virginia Lee, and Peter Seubert for tau antibodies and the Developmental Studies Hybridoma Bank (NICHD) for the β-tubulin antibody E7.

References

Alonso AC, Li B, Grundke-Iqbal I, Iqbal K. Mechanism of tau-induced neurodegeneration in Alzheimer disease and related tauopathies. Curr Alzheimer Res. 2008; 5:375–384. [PubMed: 18690834]

Arrasate M, Perez M, Armasportela R, Avila J. Polymerization of tau peptides into fibrillar structures. The effect of FTDP-17 mutations. FEBS Lett. 1999; 446:199–202. [PubMed: 10100642]

Bandyopadhyay B, Li G, Yin H, Kuret J. Tau aggregation and toxicity in a cell culture model of tauopathy. J Biol Chem. 2007; 282:16454–16464. [PubMed: 17428800]

Barghorn S, Zheng-Fischhofer Q, Ackmann M, Biernat J, von Bergen M, Mandelkow E-M, Mandelkow E. Structure, microtubule interactions, and paired helical filament aggregation by tau mutants of frontotemporal dementias. Biochemistry. 2000; 39:11714–11721. [PubMed: 10995239]

Biernat J, Gustke N, Drewes G, Mandelkow EM, Mandelkow E. Phosphorylation of Ser262 strongly reduces binding of tau to microtubules: distinction between PHF-like immunoreactivity and microtubule binding. Neuron. 1993; 11:153–163. [PubMed: 8393323]

Boeddrich A, Lurz R, Wanker EE. Huntingtin fragments form aggresome-like inclusion bodies in mammalian cells. Methods Mol Biol. 2003; 232:217–229. [PubMed: 12840552]

Boland B, Kumar A, Lee S, Platt FM, Wegiel J, Yu WH, Nixon RA. Autophagy induction and autophagosome clearance in neurons: relationship to autophagic pathology in Alzheimer's disease. J Neurosci. 2008; 28:6926–6937. [PubMed: 18596167]

Carmel G, Mager EM, Binder LI, Kuret J. The structural basis of monoclonal antibody Alz50's selectivity for Alzheimer's disease pathology. J Biol Chem. 1996; 271:32789–32795. [PubMed: 8955115]

David DC, Layfield R, Serpell L, Narain Y, Goedert M, Spillantini MG. Proteasomal degradation of tau protein. J Neurochem. 2002; 83:176–185. [PubMed: 12358741]

Debure L, Vayssiere JL, Rincheval V, Loison F, Le Drean Y, Michel D. Intracellular clusterin causes juxtanuclear aggregate formation and mitochondrial alteration. J Cell Sci. 2003; 116:3109–3121. [PubMed: 12799419]

Ding H, Dolan PJ, Johnson GV. Histone deacetylase 6 interacts with the microtubule-associated protein tau. J Neurochem. 2008; 106:2119–2130. [PubMed: 18636984]

Evans DB, Rank KB, Bhattacharya K, Thomsen DR, Gurney ME, Sharma SK. Tau phosphorylation at serine 396 and serine 404 by human recombinant tau protein kinase II inhibits tau's ability to promote microtubule assembly. J Biol Chem. 2000; 275:24977–24983. [PubMed: 10818091]

Fischer D, Mukrasch MD, Biernat J, Bibow S, Blackledge M, Griesinger C, Mandelkow E, Zweckstetter M. Conformational changes specific for pseudophosphorylation at serine 262 selectively impair binding of tau to microtubules. Biochemistry. 2009; 48:10047–10055. [PubMed: 19769346]

Gendron TF, Petrucelli L. The role of tau in neurodegeneration. Mol Neurodegener. 2009; 4:13. [PubMed: 19284597]

Goedert M, Jakes R, Crowther RA. Effects of frontotemporal dementia FTDP-17 mutations on heparin-induced assembly of tau filaments. FEBS Lett. 1999; 450:306–311. [PubMed: 10359094]

Goldbaum O, Oppermann M, Handschuh M, Dabir D, Zhang B, Forman MS, Trojanowski JQ, Lee VMY, RichterLandsberg C. Proteasome inhibition stabilizes tau inclusions in oligodendroglial cells that occur after treatment with okadaic acid. J Neurosci. 2003; 23:8872–8880. [PubMed: 14523089]

Gotz J, Ittner LM, Fandrich M, Schonrock N. Is tau aggregation toxic or protective: a sensible question in the absence of sensitive methods? J Alzheimers Dis. 2008; 14:423–429. [PubMed: 18688093]

Guthrie CR, Schellenberg GD, Kraemer BC. SUT-2 potentiates tau-induced neurotoxicity in *Caenorhabditis elegans*. Hum Mol Genet. 2009; 18:1825–1838. [PubMed: 19273536]

Hailey DW, Rambold AS, Satpute-Krishnan P, Mitra K, Sougrat R, Kim PK, Lippincott-Schwartz J. Mitochondria supply membranes for autophagosome biogenesis during starvation. Cell. 2010; 141:656–667. [PubMed: 20478256]

Hamano T, Gendron TF, Ko LW, Yen SH. Concentration-dependent effects of proteasomal inhibition on tau processing in a cellular model of tauopathy. Int J Clin Exp Pathol. 2009; 2:561–573. [PubMed: 19636403]

Hong M, Zhukareva V, Vogelsberg-Ragaglia V, et al. Mutation-specific functional impairments in distinct tau isoforms of hereditary FTDP-17. Science. 1998; 282:1914–1917. [PubMed: 9836646]

Imajoh-Ohmi S, Kawaguchi T, Sugiyama S, Tanaka K, Omura S, Kikuchi H. Lactacystin, a specific inhibitor of the proteasome, induces apoptosis in human monoblast U937 cells. Biochem Biophys Res Commun. 1995; 217:1070–1077. [PubMed: 8554559]

Ishihara T, Hong M, Zhang B, Nakagawa Y, Lee MK, Trojanowski JQ, Lee VMY. Age-dependent emergence and progression of a tauopathy in transgenic mice overexpressing the shortest human tau isoform. Neuron. 1999; 24:751–762. [PubMed: 10595524]

Iwata A, Christianson JC, Bucci M, Ellerby LM, Nukina N, Forno LS, Kopito RR. Increased susceptibility of cytoplasmic over nuclear polyglutamine aggregates to autophagic degradation. Proc Natl Acad Sci USA. 2005a; 102:13135–13140. [PubMed: 16141322]

Iwata A, Riley BE, Johnston JA, Kopito RR. HDAC6 and microtubules are required for autophagic degradation of aggregated huntingtin. J Biol Chem. 2005b; 280:40282–40292. [PubMed: 16192271]

Johnson GV. Tau phosphorylation and proteolysis: insights and perspectives. J Alzheimers Dis. 2006; 9:243–250. [PubMed: 16914862]

Johnston JA, Ward CL, Kopito RR. Aggresomes: a cellular response to misfolded proteins. J Cell Biol. 1998; 143:1883–1898. [PubMed: 9864362]

Kawaguchi Y, Kovacs JJ, McLaurin A, Vance JM, Ito A, Yao TP. The deacetylase HDAC6 regulates aggresome formation and cell viability in response to misfolded protein stress. Cell. 2003; 115:727–738. [PubMed: 14675537]

Keck S, Nitsch R, Grune T, Ullrich O. Proteasome inhibition by paired helical filament-tau in brains of patients with Alzheimer's disease. J Neurochem. 2003; 85:115–122. [PubMed: 12641733]

Khlistunova I, Biernat J, Wang YP, Pickhardt M, vonBergen M, Gazova Z, Mandelkow E, Mandelkow M. Inducible expression of tau repeat domain in cell models of tauopathy—aggregation is toxic to cells but can be reversed by inhibitor drugs. J Biol Chem. 2006; 281:1205–1214. [PubMed: 16246844]

Kosik KS, Shimura H. Phosphorylated tau and the neurodegenerative foldopathies. Biochim Biophys Acta. 2005; 1739:298–310. [PubMed: 15615647]

Nixon RA. Autophagy, amyloidogenesis and Alzheimer disease. J Cell Sci. 2007; 120:4081–4091. [PubMed: 18032783]

Oddo S. The ubiquitin–proteasome system in Alzheimer's disease. J Cell Mol Med. 2008; 12:363–373. [PubMed: 18266959]

Olzmann JA, Li L, Chin LS. Aggresome formation and neurodegenerative diseases: therapeutic implications. Curr Med Chem. 2008; 15:47–60. [PubMed: 18220762]

Perez M, Santa-Maria I, Gomez de Barreda E, et al. Tau—an inhibitor of deacetylase HDAC6 function. J Neurochem. 2009; 109:1756–1766. [PubMed: 19457097]

Seubert P, Mawal-Dewan M, Barbour R, et al. Detection of phosphorylated Ser262 in fetal tau, adult tau, and paired helical filament tau. J Biol Chem. 1995; 270:18917–18922. [PubMed: 7642549]

Shaw G, Morse S, Ararat M, Graham FL. Preferential transformation of human neuronal cells by human adenoviruses and the origin of HEK 293 cells. FASEB J. 2002; 16:869–871. [PubMed: 11967234]

Shimura H, Schwartz D, Gygi SP, Kosik KS. CHIP–Hsc70 complex ubiquitinates phosphorylated tau and enhances cell survival. J Biol Chem. 2004; 279:4869–4876. [PubMed: 14612456]

Traenckner EB, Wilk S, Baeuerle PA. A proteasome inhibitor prevents activation of NF-kappa B and stabilizes a newly phosphorylated form of I kappa B-alpha that is still bound to NF-kappa B. EMBO J. 1994; 13:5433–5441. [PubMed: 7957109]

Trojanowski JQ, Lee VM. The role of tau in Alzheimer's disease. Med Clin North Am. 2002; 86:615–627. [PubMed: 12168561]

Tsubuki S, Saito Y, Tomioka M, Ito H, Kawashima S. Differential inhibition of calpain and proteasome activities by peptidyl aldehydes of di-leucine and tri-leucine. J Biochem. 1996; 119:572–576. [PubMed: 8830056]

Wang Y, Martinez-Vicente M, Kruger U, Kaushik S, Wong E, Mandelkow EM, Cuervo AM, Mandelkow E. Tau fragmentation, aggregation and clearance: the dual role of lysosomal processing. Hum Mol Genet. 2009; 18:4153–4170. [PubMed: 19654187]

Wang Y, Martinez-Vicente M, Kruger U, Kaushik S, Wong E, Mandelkow EM, Cuervo AM, Mandelkow E. Synergy and antagonism of macroautophagy and chaperone-mediated autophagy in a cell model of pathological tau aggregation. Autophagy. 2010; 6:182–183. [PubMed: 20023429]

Yoshiyama Y, Higuchi M, Zhang B, et al. Synapse loss and microglial activation precede tangles in a P301S tauopathy mouse model. Neuron. 2007; 53:337–351. [PubMed: 17270732]

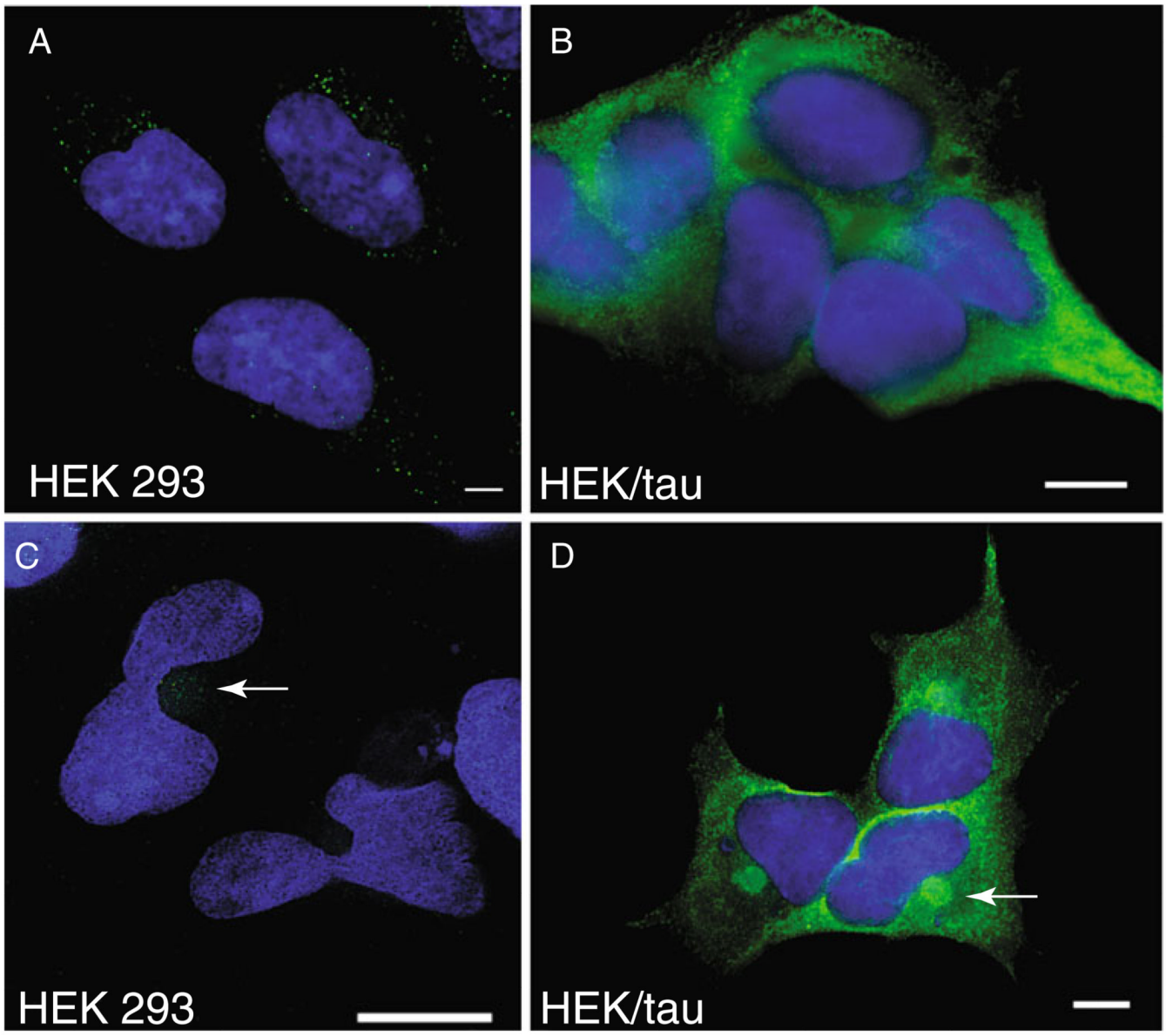

Fig. 1.

Proteasome inhibition drives aggresome formation in tau overexpressing cells. Overexpression of wild-type tau (4R1N) in HEK293 cells. Both endogenous (**a**, **c**) and stably overexpressed (**b**, **d**) tau protein are detected by immunofluorescence with tau antibody T46 (*green*). Cells treated with 2 μM PSI for 18 h (**c**, **d**) show spherical aggresome-like structures (*arrows*) at the MTOC. The nuclear compartment is counterstained with DAPI (*blue*). *Single arrow* indicates aggresomes. Note the prominent deformation of the nucleus adjacent to aggresomes. *Scale bars*=10 μm

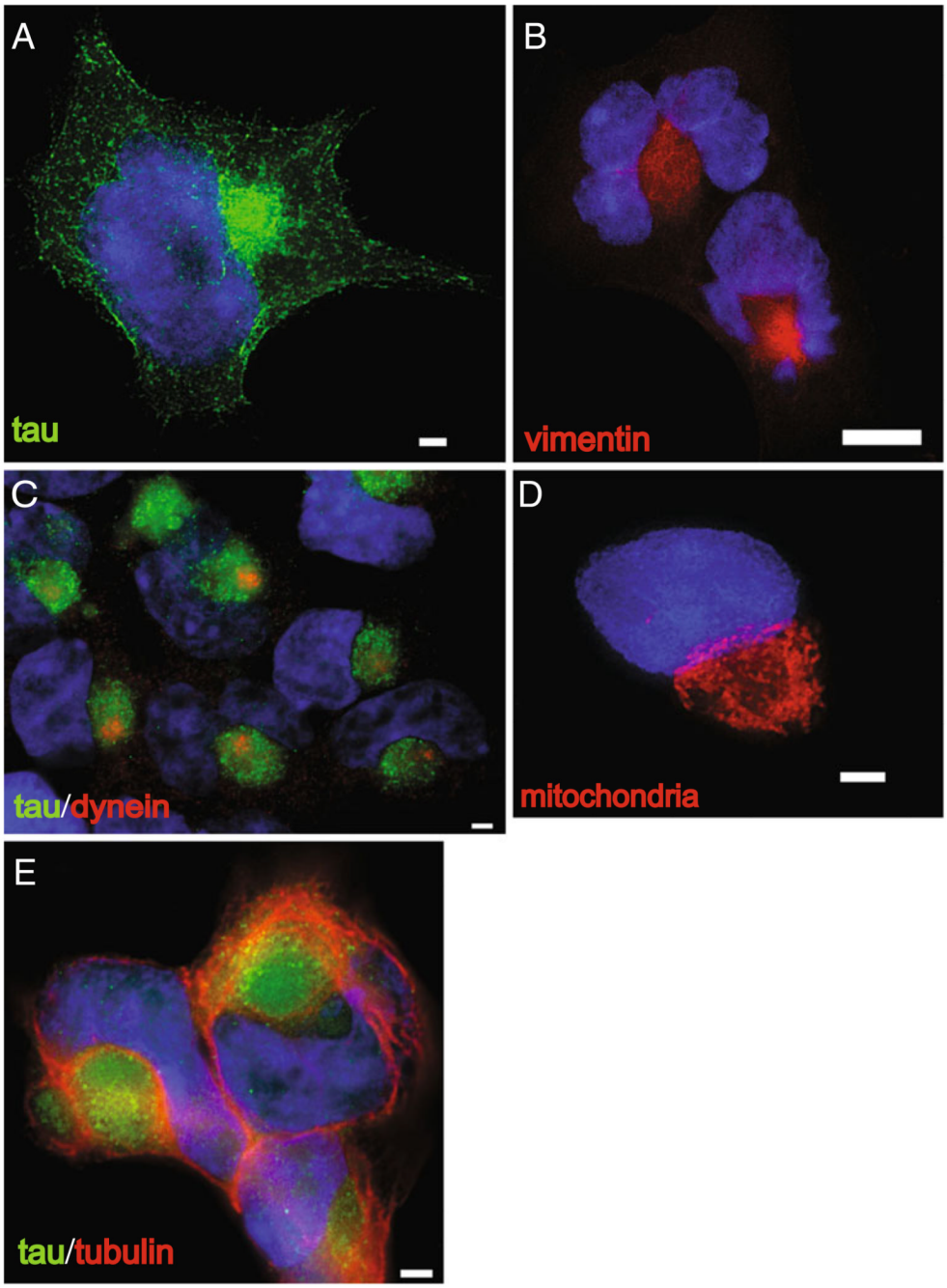

Fig. 2.

Proteasome inhibition causes tau to aggregate in structures with hallmarks of aggresomes. Treatment of HEK/tau cells with 2 μM PSI leads to accumulations characteristic of aggresomes at the MTOC. **a** Tau protein (*green*) detected with T46 antibody, **b** vimentin protein (*red*) forms a cage-like structure around the aggresome, **c** the retrograde motor protein dynein (*red*) concentrates at the centrosome, **d** mitochondria(*red*) labeled with MitoTracker dye surround the aggresome, **e** microtubules detected with β-tubulin antibody (*red*). Nuclei are labeled by staining DNA with DAPI (*blue*). *Scale bars*=10 μm

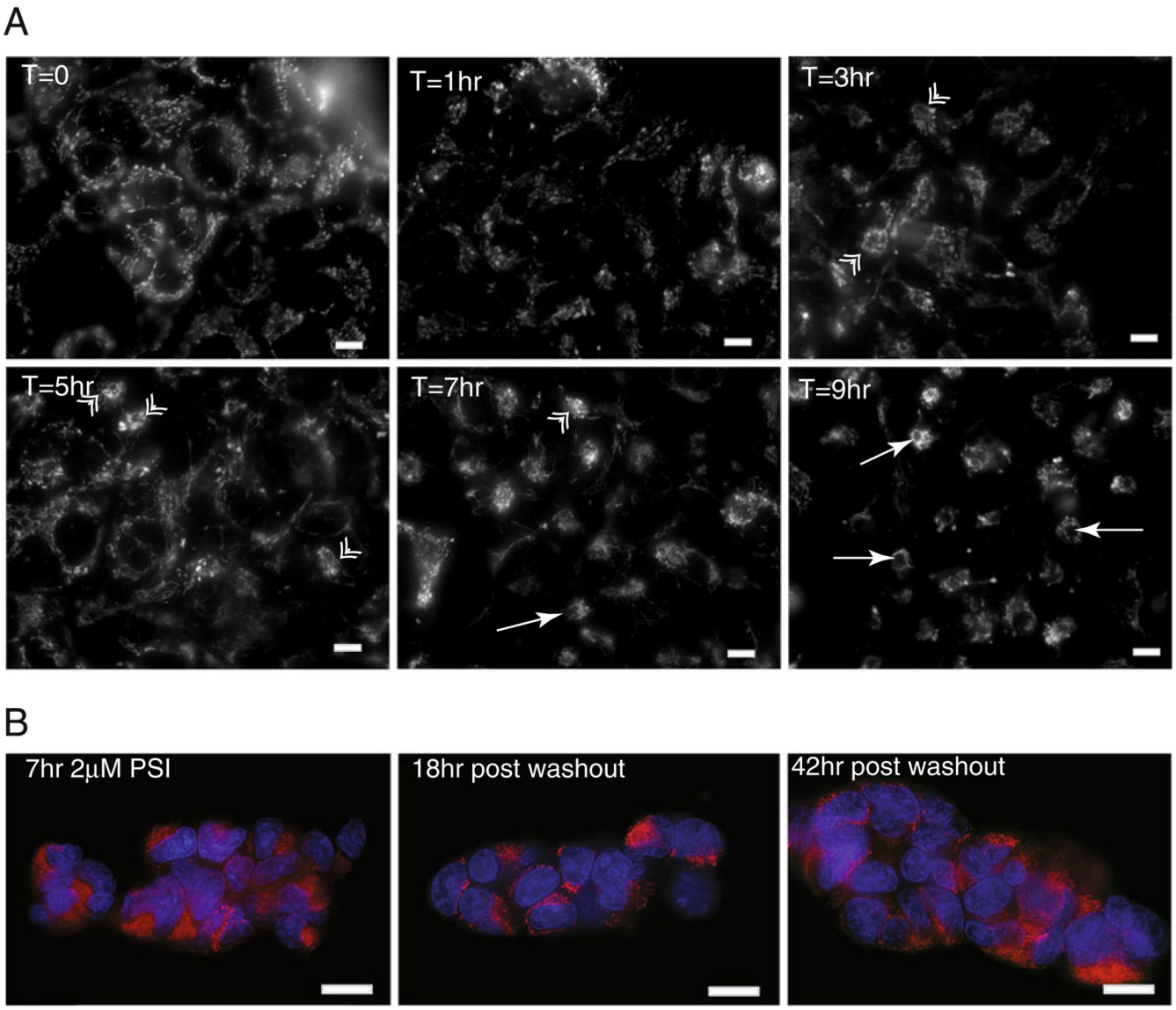

Fig. 3.

Aggresome formation begins soon after inhibition of proteasome activity and is reversible. **a** Live HEK/tau cells labeled with MitoTracker dye. Mitochondria accumulate around the aggresome at various time points after addition of 2 μM PSI. Mitochondria begin to accumulate around aggresome as early as 3 h. in a few cells (*arrows*). By 7 h, mitochondria accumulation at the MTOC is obvious, and aggresome formation is essentially complete at 9 h of treatment. *Double arrowheads* indicate nascent aggresomes; *single arrows* mark mature fully formed aggresomes. **b** Aggresomes are cleared following washout of proteasome inhibitor; 18 h after washout of proteasome inhibitor, mature aggresomes are beginning to clear as indicated by a more regular distribution of mitochondria (*red*) throughout the cytoplasm. At 42 h post-washout, mitochondrial distribution appears much as in *T*=0. The nuclear compartment is counterstained with DAPI (*blue*). *Scale bars*=10 μm

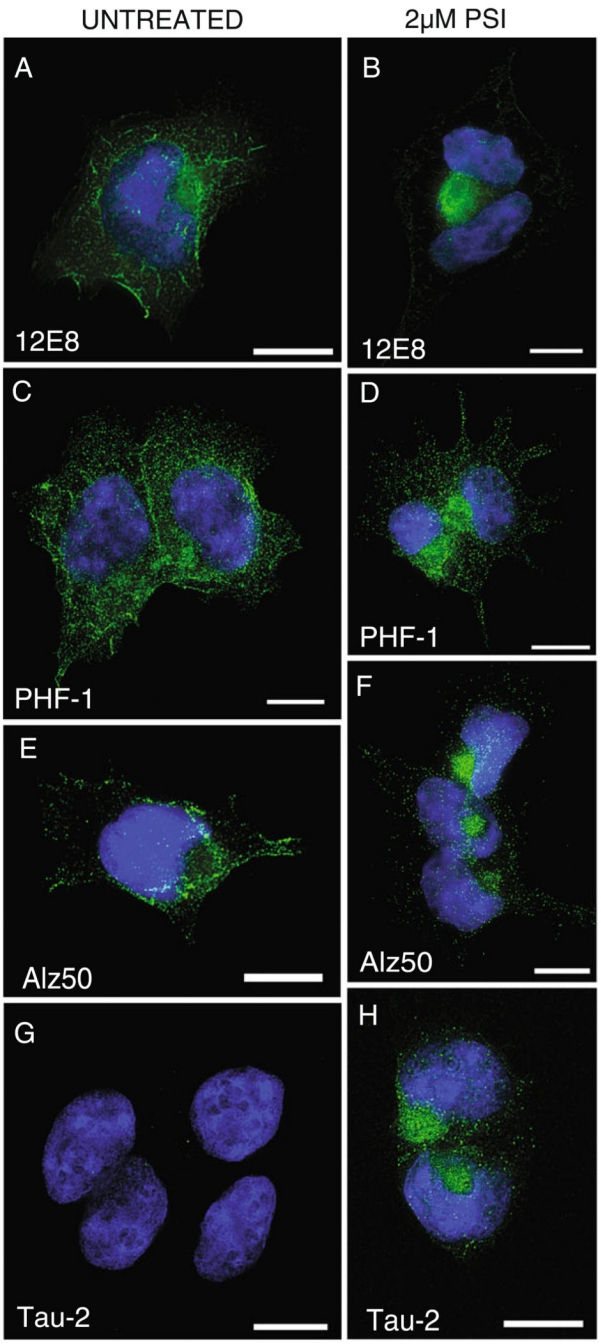

Fig. 4.

Pathological tau is recruited to aggresomes in HEK/tau cells. PSI-treated cells (**b**, **d**, **f**, **h**) are compared to untreated cells (**a**, **c**, **e**, **g**). **a**, **b** Stained with antibody 12E8 (recognizes phospho-Ser262); **c**, **d** PHF-1 (recognizes phospho-Ser396/404); **e**, **f** Alz50 (recognizes pre-tangle conformations of PHF tau); **g**, **h** tau-2 (preferentially binds PHF related conformations of tau). In all panels, tau antibody stain is *green*, and nuclei are labeled with DAPI (*blue*). *Scale bars*=10 μm

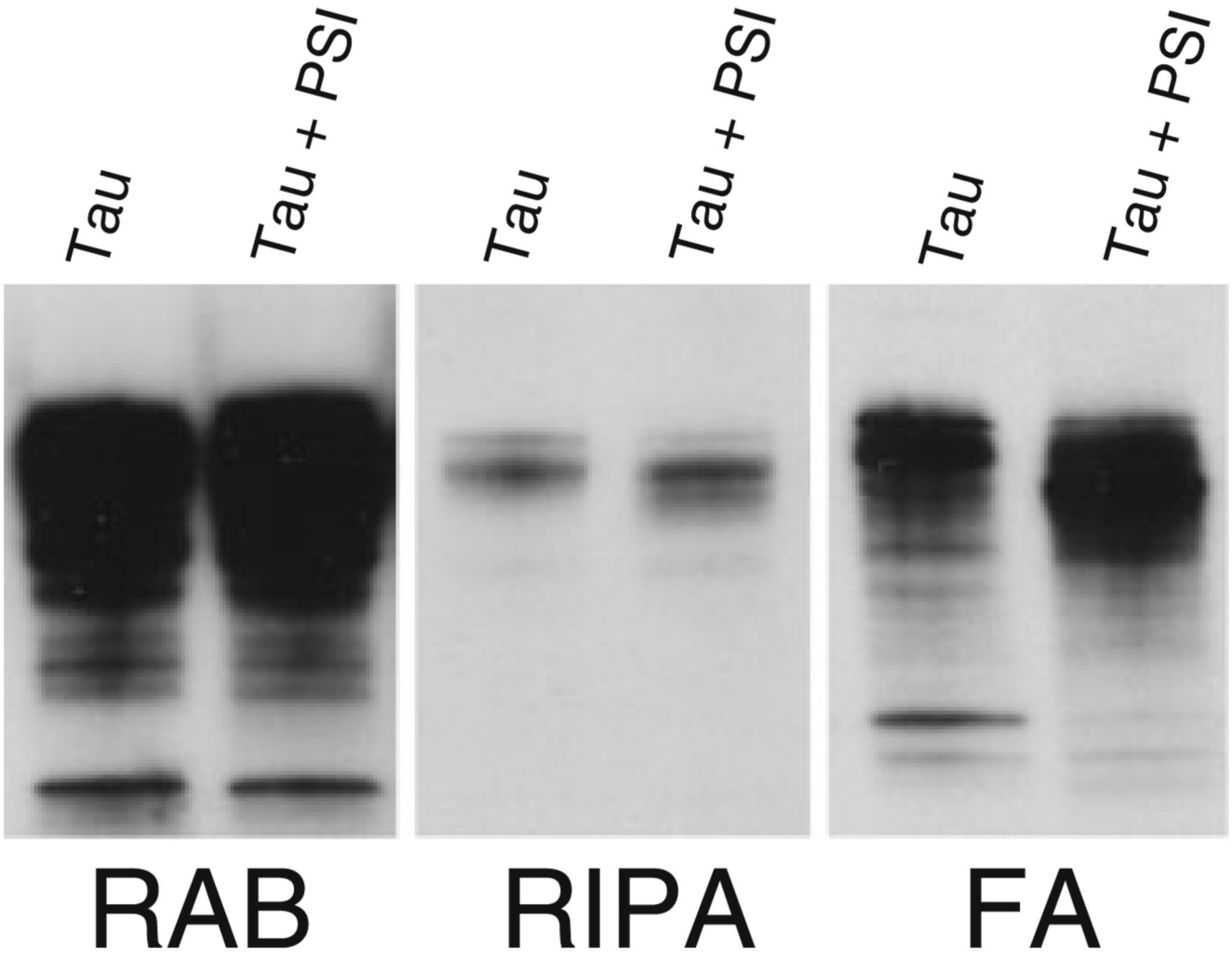

Fig. 5.

Aggresome formation drives additional accumulation of insoluble tau. Tau protein was sequentially extracted to obtain detergent insoluble tau protein from HEK/tau cells with or without PSI treatment. RAB contains tau solubilized by high salt; RIPA contains detergent soluble tau, while FA contains the detergent insoluble material FA solubilized protein. *Tau* untreated HEK/tau cell extracts, *Tau + PSI* HEK/tau cells treated with 2 μM PSI for 18 h

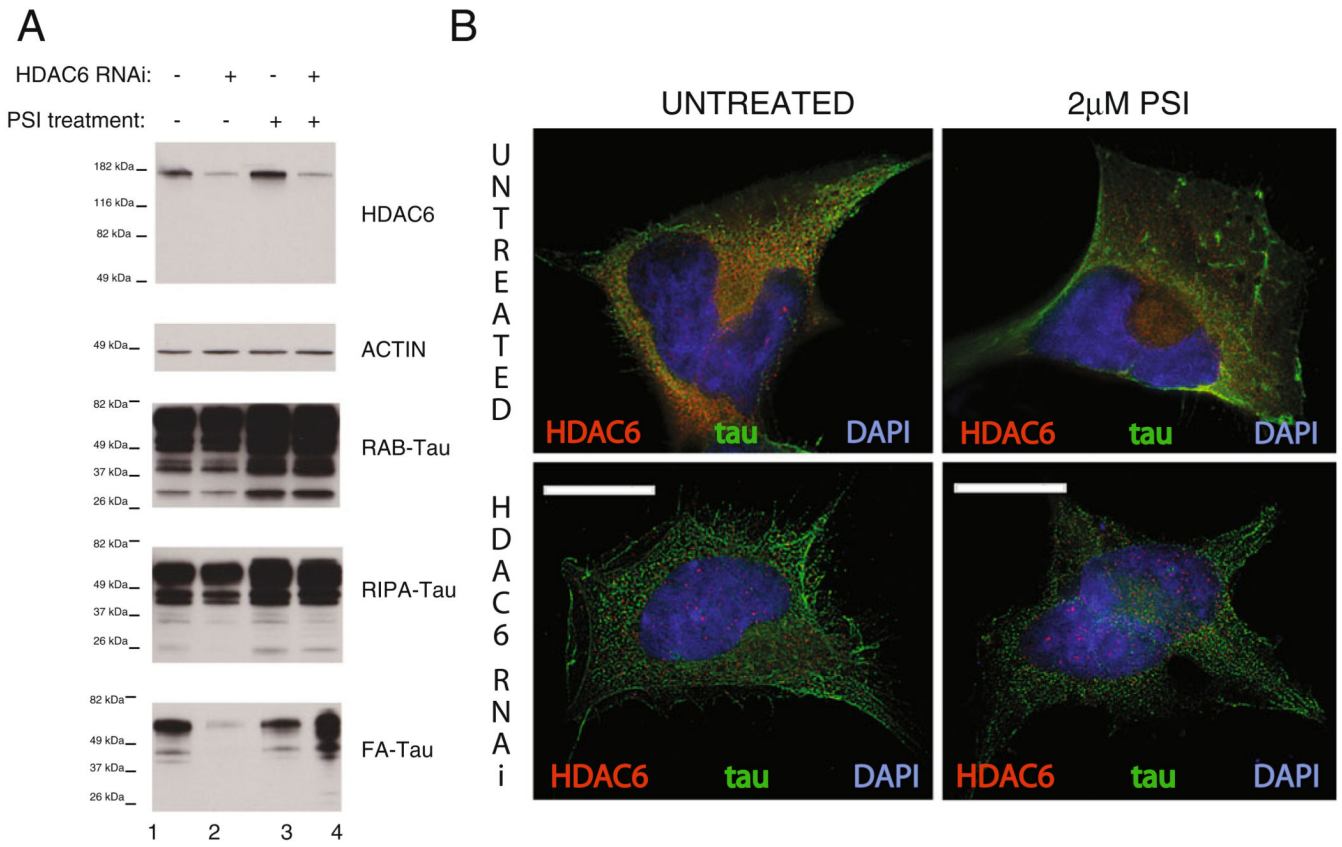

Fig. 6.

HDAC6 levels and the proteasome control tau aggregation and toxicity. **a** Tau protein was sequentially extracted to obtain detergent insoluble tau protein from HEK/tau cells with or without PSI treatment. RAB contains tau solubilized by high salt; RIPA contains detergent soluble tau, while FA contains the detergent insoluble material solubilized by FA extraction. PSI treatment indicates HEK/tau cells treated with 2 μM PSI for 18 h. RNAi treatment occurs prior to PSI treatment and consists of overnight exposure of cells to siRNA duplexes that target HDAC6 followed by 72 h growth. **b** Untreated HEK/tau cells immunostained for HDAC6 and tau display typical translocation of tau along with HDAC6 to the aggresome upon treatment with 2 μM PSI for 18 h. HDAC6 siRNA treatment, however, inhibits formation of the aggresome when proteasome activity is compromised. *Scale bars*=10 μm